Algal Research
November 2018, Volume 35 Pages 508-518
https://doi.org/10.1016/j.algal.2018.09.023
https://archimer.ifremer.fr/doc/00460/57133/

Allelochemicals from *Alexandrium minutum* induce rapid inhibition of metabolism and modify the membranes from *Chaetoceros muelleri*

Long Marc [1, 2, *], Tallec Kevin [3], Soudant Philippe [1], Le Grand Fabienne [1], Donval Anne [1], Lambert Christophe [1], Sarthou Géraldine [1], Jolley Dianne F. [2], Hégaret Helene [4]

[1] Laboratoire des Sciences de l'Environnement Marin (LEMAR), UMR 6539 CNRS UBO IRD IFREMER – Institut Universitaire Européen de la Mer, Technopôle Brest-Iroise, Rue Dumont d'Urville, 29280 Plouzané, France
[2] School of Chemistry, University of Wollongong, NSW 2522, Australia
[3] Ifremer, Laboratoire des Sciences de l'Environnement Marin (LEMAR), UMR 6539 UBO/CNRS/IRD/Ifremer, 29280 Plouzané, France

* Corresponding author : Marc Long, email address : marc.florian.long@gmail.com

Abstract :

Allelochemical interactions are likely to be a contributing factor explaining the success of large blooms of the harmful marine dinoflagellate *Alexandrium*, however, the physiological mechanisms of allelochemical interactions remain poorly described. Here we investigated the sub-lethal effects (on an hourly scale) of a filtrate containing allelochemicals from *Alexandrium minutum* on the physiology of the common diatom *Chaetoceros* muelleri. The filtrate induced deleterious effects to the diatom physiology within only 30 min of exposure. Esterase activity and photosynthesis were drastically inhibited, with up to 34% of the population being metabolically inactive and up to 30% reduction in photosystem II quantum yield when exposed to the filtrate. In addition, intracellular reactive oxygen species increased by 26% in response to allelochemical exposure. *C. muelleri* pigment and lipid analyses indicated that the photosystem II was inhibited, with photoinhibition-like responses (activation of xanthophyll cycles, and changes in associated lipids) upregulated to mitigate the toxic effects of allelochemicals. Changes in the proportions of membrane lipid classes and increased membrane fatty acids saturation by 9% may be an attempt to maintain membrane integrity and associated enzyme activity, or could be the result of deleterious effects on membranes. An 8% decrease in cellular storage lipids (triglycerides) revealed a mobilization of energy suggesting an energetic cost for the diatom to counteract the allelochemical effects. We hypothesize that the rapid alteration of physiological functions such as photosynthesis and some enzymatic activities may result from direct damage on external membranes. Overall this study describes the sub-lethal mechanisms and provides useful biomarkers to understand the role of allelochemical interactions and associated ecological processes in structuring plankton communities.

Highlights

► Allelochemicals released by *Alexandrium minutum* are fast acting compounds. ► This study describes the sub-lethal mechanisms induced by *A. minutum* allelochemicals. ► Allelochemicals change the biochemistry of *Chaetoceros* sp. membranes. ► Allelochemicals inhibit photosynthesis and induce photoinhibition-like responses. ► Allelochemicals increase ROS production and inhibit primary metabolism.

Keywords : Allelopathy, Alexandrium, Metabolism, Photoinhibition, Lipids, Pigments

1 Introduction

The structure of plankton communities is shaped by complex interactions with their environment. The influence of abiotic factors, such as light, nutrients, seawater or stratification are well studied and known to have a strong role in community structure. The roles of biotic factors however are less well understood despite the increasing evidence that biotic factors are shaping plankton communities (Lima-Mendez et al., 2015; Worden et al., 2015). Chemical interactions between organisms (i.e. chemical ecology) are influencing the structure of marine communities. Chemical compounds can mediate communication between microbes, can play a role in sexual reproduction and competition between species or can be a chemical defense against grazers and pathogens (Ianora et al., 2006; Pohnert, 2010; Puglisi et al., 2014). Within this field, allelochemical interactions refer to the beneficial or adverse effects of chemicals (allelochemicals) released by a protist on the biology of co-occurring protists, predators or bacterial cells. The release of toxic allelochemicals gives the donor species a competitive advantage that could result in the formation of large blooms (Granéli et al., 2006; Legrand et al., 2003).

The genus *Alexandrium* is known to produce uncharacterized extracellular compounds with potent allelochemical activity. It is hypothesized that the allelochemical potency of this genus may enhance the establishment of large *Alexandrium* spp. blooms (Tillmann and Hansen, 2009). The allelochemical potency is widespread among the genus *Alexandrium* as this activity was shown in at least 9 species: *A. minutum, A. fundyense, A. lusitanicum, A. affine, A. ostenfeldii, A. pseudogonyaulax, A. tamarense, A. taylori and A. tamutum* (Blanco and Campos, 1988; Lelong et al., 2011; Lyczkowski and Karp-Boss, 2014; Tillmann et al., 2016; Tillmann and John, 2002). Allelochemicals are released by cells into the surrounding environment and within minutes to hours induce cell lysis, cell immobilization and cyst formation (Tillmann et al., 2007). Furthermore some of these allelochemicals may be responsible for other toxic effects on mammalian erythrocytes (Arzul et al., 1999), and bivalve gametes (Le Goïc et al., 2014). They may also be responsible for reduced growth and behavior modification of the great scallop *Pecten maximus* (Borcier et al., 2017) or deleterious effects on the physiology of the oyster *Crassostrea gigas* (Castrec et al., 2018). Nevertheless the nature and mode of action of those extracellular compounds remain unknown.

Researchers studying allelochemical interactions often quantify their effects on microalgal growth rate, membrane permeability and cell lysis in target cells however very few studies

precisely elucidate the mode of action. For example, studies exploring allelochemical mechanisms from the genus *Alexandrium* have investigated their effects on photosynthesis (Lelong et al., 2011), membranes (Ma et al., 2011) and transcriptomic (Zheng et al., 2016), however the story is still incomplete. While the long-term (i.e. mainly lethal) effects are fairly well described, the short-term (i.e. sub-lethal) effects and cellular processes leading to cell death remain unclear. More specifically, the effects of allelochemicals on the biochemical composition of membranes, that seem to have a central role in allelochemical sensitivity (Ma et al., 2011) are unknown.

The aim of this study was to elucidate the mechanistic effects (at a subcellular level) of allelochemicals released by *Alexandrium minutum* on the common diatom *Chaetoceros muelleri* a diatom co-occurring with *A. minutum* (Chapelle et al., 2014). The study focused on the photosynthetic apparatus and biochemistry of membranes. Allelochemicals were separated from *A. minutum* cells by filtration to specifically focus on allelochemical interactions and avoid interference by cell-cell interactions. A pulse of allelochemicals was performed to study the short-term sub-lethal effects of allelochemicals on *C. muelleri*, measuring the effects on photosynthesis, intracellular reactive oxygen species production and esterase activity, a proxy of primary metabolism (Brookes et al., 2000; Dorsey et al., 1989). To further explore the allelochemical interactions at the membrane level, we analyzed the membrane composition of the diatom (polar lipid classes, fatty acids composition of polar lipids, and sterol content) and pigments after 30 and 60 min of exposure to the filtrate. Neutral lipids classes were also analyzed to detect free fatty acid increases as a cell lysis indicator or a decrease of storage lipids (triacylglycerols) as a stress response.

2 Materials and methods

2.1 Microalgal cultures

A strain of *Alexandrium minutum* (strain CCMI1002, isolated from a bloom in Gearhies, Bantry Bay, Ireland; Touzet et al., 2007), not producing paralytic shellfish toxins (PST), was selected according to its high allelochemical potency (Borcier et al., 2017). The dinoflagellates were cultivated in triplicate for 10 days in 1 L of autoclaved L1 media (Guillard, 1975) prepared with natural filtered (0.2 µm) seawater from Argenton, France (Salinity = 34 psu, pH = 8.4) a pristine site for *Alexandrium* spp. Cultures of *A. minutum* were maintained in exponential growth phase to obtain a concentration of 9.6 x 10^4 cells mL^{-1} on the experimental day (growth rate: 0.18 day^{-1}). A strain of *Chaetoceros muelleri* (strain CCAP 1010-3 obtained from the CCAP culture collection, formerly listed as *Chaetoceros neogracile*

or *Chaetoceros* sp.) was selected because of its sensitivity to *A. minutum* allelochemicals (Borcier et al., 2017; Lelong et al., 2011) and because of the ubiquity of its genus in phytoplankton communities (Dalsgaard et al., 2003). Cultures of the diatom were grown for 10 days (2.12 x 10^6 cells mL^{-1}) in 6 L of autoclaved synthetic ocean seawater (Morel et al., 1979) enriched with L1 media (salinity = 35 psu, pH = 8.4) and silicate (1.06 x 10^{-4} M). Cultures of *C. muelleri* were in late exponential growth phase on the day of the experiment (growth rate: 0.15 day^{-1}). All cultures were maintained at 18 °C under a continuous light intensity of 100 – 110 µmol photon m^{-2} s^{-1}. Cultures were not axenic but were handled under sterile conditions to minimize additional bacterial contamination.

2.2 Exposure to allelochemicals

Allelochemicals were separated from cultures by centrifugation (10 min, 800 g, 18 °C) followed by a filtration (0.2 µm, Minisart syringe filter, acetate cellulose membrane, 16534-K, Sartorius) of supernatant (Lelong et al., 2011). The filtrate concentrations were expressed as cell concentration (cells mL^{-1}) based on the initial culture concentration prior to filtration. Cultures of *C. muelleri* in late exponential growth phase were diluted to 1.38 x 10^6 cells mL^{-1} with filtered seawater and distributed to six 2 L glass balloon flasks. The diatom *C. muelleri* was then exposed in triplicate to two different conditions for 90 min: i) 12 mL of *A. minutum* filtrate (final concentration from 1200 *A. minutum* cells mL^{-1}), ii) the same volume (12 mL) of filtered seawater as a control (final volume in each condition 1 L). During the exposure (maximum 90 min), the flasks were kept under ambient laboratory light and temperature conditions (not measured).

2.3 Photosynthetic parameters

Photosynthetic measurements were performed by pulse amplitude modulation (PAM) fluorometry using an AquaPen-C AP-C 100 with a blue light (455 nm). Sub-samples of *C. muelleri* were dark-adapted for at least 10 min, allowing the full oxidation of photosystem II (PSII) reaction centers and electron chain transport, before the measurement of fluorescence variables and PSII maximum quantum yield ($Fv/Fm = (F_m - F_0) / F_m$). F_0 is the initial fluorescence intensity, and F_m the maximal intensity under saturating light (Strasser et al., 2000). Measurement of fluorescence variables were performed every 10 min for 100 min following the exposure.

Non-photochemical quenching (NPQ) measurements were performed in a separate experiment. Six replicates of the diatom *C. muelleri* (2 x 10^5 cells mL^{-1}) in exponential

growth phase were exposed for 45 min to *A. minutum* filtrate (final *A. minutum* concentration of 6 x 10^3 cells mL^{-1}). The cells of *C. muelleri* were exposed to three successive flashes of 60 s (saturated light, 3 000 µmol photons m^{-2} s^{-1}) and 3 dark phases of 80 s for NPQ measurements, in the presence of filtered seawater or filtrate.

2.4 Flow-cytometry measurements

Population growth counts and measurements of phytoplanktonic cell variables were performed using a FACScalibur (BD Biosciences, San Jose, CA, USA) flow cytometer with a 488 nm argon laser. Counts were estimated according to flowrate (Marie et al., 1999). Cell variables, e.g. forward scatter (Forward scatter, FSC), side scatter (Side scatter, SSC) and red autofluorescence (Fl3, red emission filter long pass, 670 nm) were used to select diatom population. All flow cytometry measurements on *C. muelleri* (cell variables, esterase activity and reactive oxygen species production) were performed after 30, 60 and 90 min of exposure to *A. minutum* filtrate or filtered seawater.

Microalgal esterase activity, a proxy of primary metabolism was assessed with fluorescein diacetate staining (FDA; Invitrogen # F1303; at a final concentration of 6 µM) (Brookes et al., 2000; Dorsey et al., 1989; Franklin et al., 2001; Garvey et al., 2007). FDA is a nonpolar compound that can permeate into the cells. Once inside the cells, FDA is cleaved by esterases into acetate and fluorescein molecules (emission wavelength 525 nm), which are retained within the cells. Intracellular concentrations increase with both metabolic activity and time. Samples were incubated with the stain for precisely 10 min in the dark prior to flow-cytometry measurements. Intracellular fluorescence intensity, which is proportional to the amount of FDA cleaved by esterases within the cells, was measured with Fl1 emission filter (green emission filter band pass, 530/30 nm). Cell populations of *C. muelleri* could be divided into 3 sub-populations: cells with highest Fl1 fluorescence corresponding to high esterase activity (metabolically active), cells with a low Fl1 fluorescence corresponding to cells with reduced esterase activity (reduced metabolism), and cells which Fl1 fluorescence equivalent to microalgal auto-fluorescence from cells with inactive esterases (metabolically inactive). Results were expressed as the percentages of cells with high esterase activity, cells with low reduced esterase activity and cells with inactive esterases.

Intracellular reactive oxygen species (ROS) production was measured using 2',7'-dicholorofluorescindiacetate (DCFH-DA; Sigma-Aldrich, D6883; at a final concentration of 10 µM). DCFH-DA is a cell-membrane permeable fluorescent stain that is a proxy of ROS production. Once inside the cells, DCFH-DA is hydrolyzed by esterase to form the non-

fluorescent DCFH retained within the cell. DCFH can thus be oxidized by H_2O_2 and other oxidants to produce fluorescent 2',7'-dicholorofluorescin (DCF). Intracellular oxidation levels were correlated to DCF fluorescence within the cells and measurable by flow cytometry with Fl1 emission filter (green emission filter band pass, 530/30 nm). Samples were incubated with the stain for 20 min in the dark prior to flow-cytometry measurements. The relative ROS production is expressed as the mean Fl1 fluorescence per cell.

2.5 Pigments extraction and composition

For pigment analysis, 3.4 x 10^7 cells (25 mL of culture) of *C. muelleri* exposed to the filtrate or seawater were filtered over glass fiber filters (0.2 µm, Whatman GF/F) after 30 and 60 min of exposure. Pigments were extracted from cells using methanol and analyzed by high-performance liquid chromatography (HPLC) according to the method described by (Ras et al., 2008), adapted from (Van Heukelem and Thomas, 2001). All the pigment standards were purchased from DHI (HØRSHOLM, Denmark).

2.6 Lipid analysis

For lipid class and fatty acid analyses, 3.4 x 10^8 cells (250 mL of culture) of the diatom were filtered over glass fiber filters (0.2 µm Whatman GF/F filters were heated for 6 h at 450 °C prior to use) after 30 and 60 min of exposure. Boiling water was immediately passed through the filter after filtration to inhibit lipase activity. Lipids were then extracted with chloroform: methanol (2:1; v:v). Lipid extracts were stored at -20°C under nitrogen ($N_{2(g)}$) until analysis. Lipid class composition analyses were performed by high-performance thin layer chromatography (HPTLC) using a CAMAG auto-sampler to spot the sample on HPTLC glass plates pre-coated with silica gel (Merck & Co., Ltd., Darmstadt, Germany). Neutral and polar lipid classes were analyzed according to (Moutel et al., 2016). For polar and neutral lipid fatty acid (FA) analysis, an aliquot of the chloroform: methanol (2:1, v:v) extract was dried under $N_{2(g)}$ and then resuspended in chloroform:methanol (98:2, v:v) prior to neutral and polar lipid separation. Separation of neutral and polar lipids was realized by solid phase extraction (Le Grand et al., 2014). Each fraction (polar and neutral lipids) was transesterified and the resulting fatty acid methyl esters (FAME) were analyzed and quantified by gas chromatography (GC-FID) according to the method from (Le Grand et al., 2014). Lipid class and fatty acid standards were the same standards used in (Le Grand et al., 2014). FA were expressed as percentage of total FA in polar and neutral lipids. The level of unsaturation was

calculated from the % FA derived from the gas chromatographic data according to the equation:

$$Unsaturation\ level\ = \sum [\%\ of\ fatty\ acid\ \times number\ of\ double\ bond]$$

2.7 Statistics

All statistical analyses were performed using R software (R Foundation for Statistical Computing, Vienna, 2011). A generalized linear model (Glm) was performed to evaluate the influence of time, *A. minutum* filtrate and their interaction on the maximum photosystem II quantum yield (*Fv/Fm*) of *C. muelleri*. The effects of filtrate on the different physiological and biochemical parameters (NPQ, flow-cytometry measurements, pigments, lipid classes and fatty acid composition) were assessed at each time. Statistical differences between seawater and filtrate were analyzed by a Student t-test after checking homoscedasticity assumption with a Bartlett test. When not meeting homoscedasticity assumption, metabolic activity (as a percentage of cells) was transformed with square root transformations. When homoscedasticity could still not be met, a non-parametric Wilcoxon test was applied. The Bray-Curtis similarity matrix was used for a one-way analysis of similarities (ANOSIM) to test whether samples within polar and neutral lipid fractions were clustered by condition (after 30 or 60 min exposures). ANOSIM calculated a global R statistic that weighs the differences between groups, with R = 1, R = 0.5 and R = 0 indicating a perfect, satisfactory, and poor separation of the clusters, respectively (da Costa et al., 2017; González-Fernández et al., 2016). Principal component analyses (PCA) were performed to investigate the variation in fatty acid profile in *C. muelleri* exposed to seawater or to the allelochemicals after 30 or 60 min. Fatty acid (FA) data was analyzed with a similarity percentage analysis (SIMPER) performed on the relative FA content to identify the FAs accounting for 80% of dissimilarity between the groups and were shown on the PCA. All results are presented as mean ± standard deviation (n = 3). Graphs were performed with the R package ggplot.

3 Results

3.1 Pulse Amplitude Modulated fluorescence

Overall, *Fv/Fm* strongly decreased during the exposure time in presence of the filtrate (Figure 1). The filtrate of *A. minutum* rapidly (< 20 min) modified *C. muelleri* maximum photosystem II quantum yield. Allelochemicals in the filtrate induced a temporary increase in *Fv/Fm* in the first 10 min of exposure compared to the controls. Following this, *Fv/Fm* steadily decreased

to 0.41 ± 0.02 (27% inhibition) at 60 min, then increased to 0.45 ± 0.03 (20 % inhibition) after 100 min. In parallel, *Fv/Fm* from the seawater control culture remained stable between 0.58 and 0.56. After 45 min of exposure to *A. minutum* filtrate, non-photochemical quenching increased two-fold in filtrate exposures compared to controls (Figure 2).

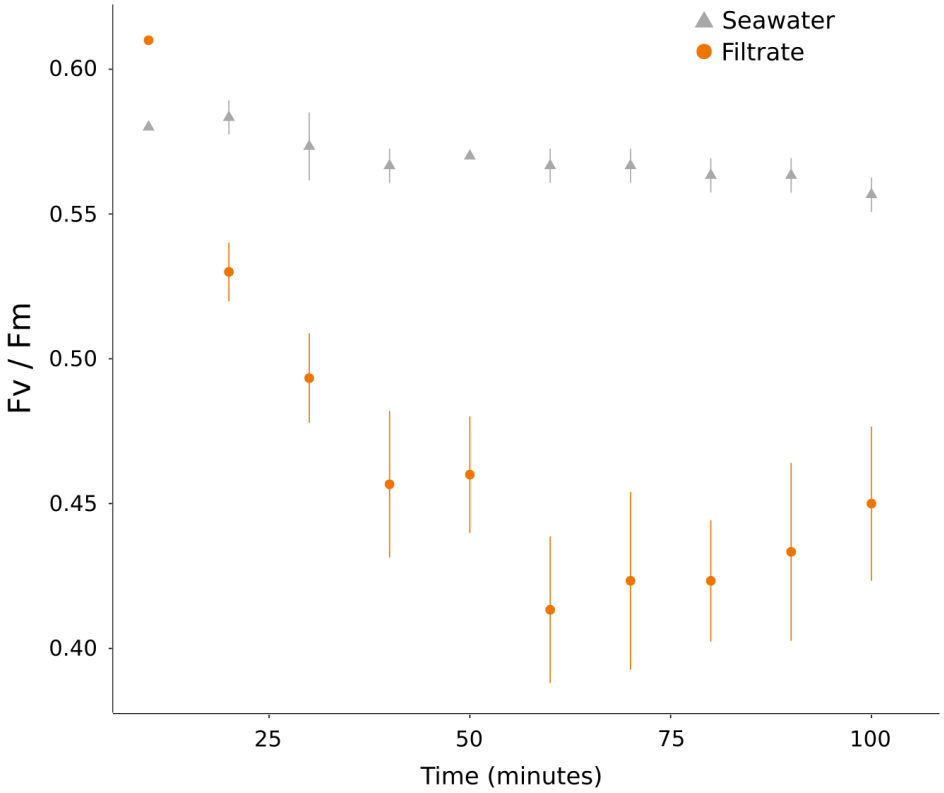

Figure 1: Maximum photosystem II quantum yield *(Fv/Fm)* of *C. muelleri* exposed to filtered seawater (grey triangles) and to *A. minutum* filtrate (orange dots). *Fv/Fm* significantly decreased over time (Glm t value = 7.469, p-value < 0.001) and a significant influence of the interaction between time and filtrate (Glm t value = -5.281, p-value < 0.001). Error bars represent the standard deviation (n = 3).

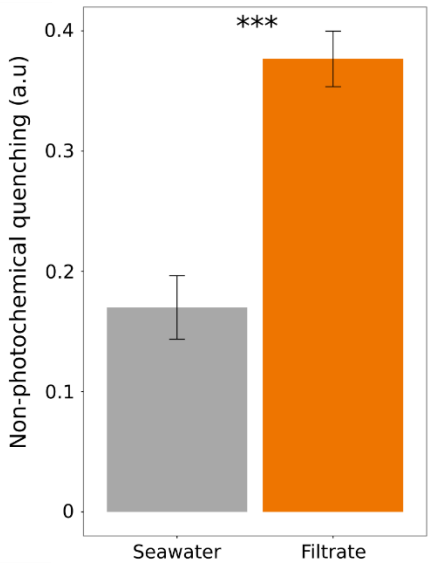

Figure 2: Non-photochemical quenching (NPQ; arbitrary unit) of *C. muelleri* after 45 min exposure to filtered seawater (control, grey bar) or *A. minutum* filtrate (orange bar) at a theoretical cell concentration equivalent to 6×10^3 cells mL^{-1}. Error bars represent the standard deviation (n = 3). ***refers to a significant difference (p-value < 0.001) between the control (seawater) and the filtrate.

3.2 Flow-cytometry parameters

Forward scatter (FSC; Figure 3A) of *C. muelleri* exposed to filtrate significantly decreased from 74.7 ± 0.6 to 67.2 ± 0.5 (arbitrary unit; a.u.) and 67.7 ± 8.7 a.u. to 43.8 ± 1.2 a.u. as compared to control after 60 and 90 min, respectively. Side scatter (SSC; Figure 3B) significantly decreased from 60.6 ± 8.3 a.u. (seawater) to 45.8 ± 0.5 a.u. (filtrate) after 90 min of exposure. Chlorophyll auto-fluorescence, as estimated by Fl3 fluorescence (Figure 3 C), steadily and significantly decreased in the cultures exposed to the filtrate compared the control cultures. After 30 min, Fl3 decreased from 1430 ± 9 a.u. in the control (seawater) to 1298 ± 19 a.u. with the filtrate (9% reduction). Fl3 fluorescence further decreased after 60 and 90 min when the inhibition reached 21 and 35%, respectively (1285 ± 122 a.u. for the control and 837 ± 44 a.u. when exposed to filtrate). A significant increase in intracellular ROS production (i.e. Fl1 fluorescence; Figure 3D) in the diatom cells was observed once exposed to filtrate. ROS production increased from 6.1 ± 0.3 a.u. in the control to 7.7 ± 0.5 a.u. when exposed to the filtrate for 30 min (26 % increase). ROS production kept increasing until 60 min to 9.5 ± 0.2 a.u. (63 % increase compared to the control at 5.8 ± 0.1 a.u. for the control), but by 90 min exposure, the ROS production from the exposed cells returned to control levels, 5.0 ± 0.1 a.u. and 5.2 ± 0.7 a.u., respectively.

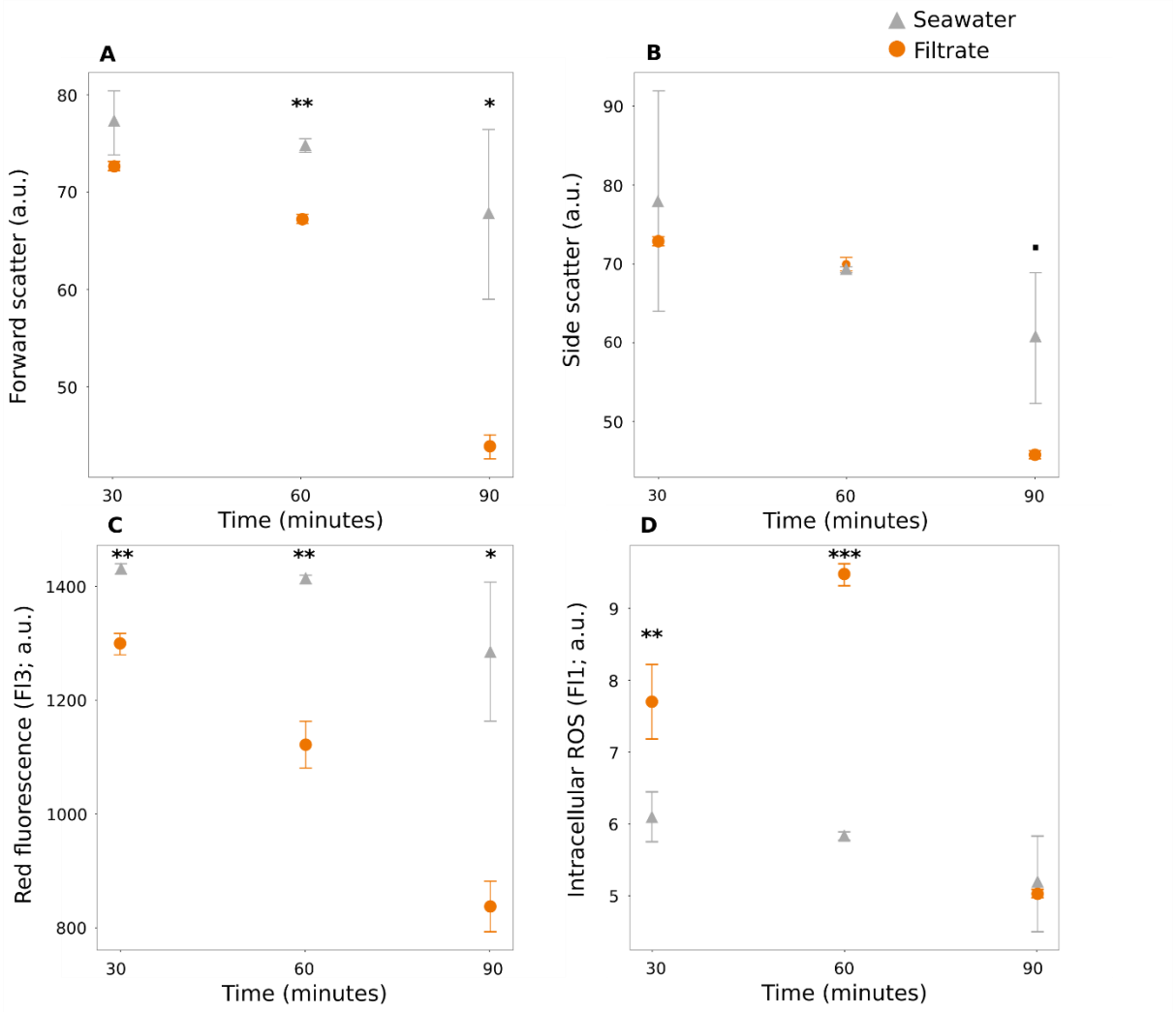

Figure 3 *:* Flow-cytometry parameters of *C. muelleri* for controls (seawater; grey triangles) and after exposure to *A. minutum* filtrate (orange dots) for 30, 60 and 90 min. A: Forward scatter (FSC), B: Side scatter (SSC), C: Fl3: red fluorescence, D: Reactive Oxygen Species (ROS) as measured by Fl1 fluorescence after DCFH-DA staining. Results are expressed as mean ± standard deviation (n = 3). Statistical differences between seawater and filtrate at each different time are indicated as followed "." 0.05 < p-value < 0.1, "*" 0.01 < p-value < 0.05, "**"0.001 < p-value < 0.01, "***" p-value < 0.001.

Filtrate of *A. minutum* significantly increased the proportion of diatom cells with a reduced esterase activity (i.e. reduced metabolic activity) and cells with inactive esterases (i.e. no metabolic activity) compared to controls (Figure 4). The cells with a reduced esterase activity represented 25 ± 4 % of the population at 30 min and reached a plateau of 34 ± 5 % after 60 min of exposure. In the control culture, this population stayed below 4 ± 1 % throughout the 90 min bioassay. Some cells had no esterase activity in cultures exposed to *A. minutum* filtrate, while in controls all cells presented esterase activity. The proportion of cells with no esterase activity increased from 3 ± 1 % to 10 ± 2 % and 13 ± 1 % at 30, 60 and 90 min, respectively.

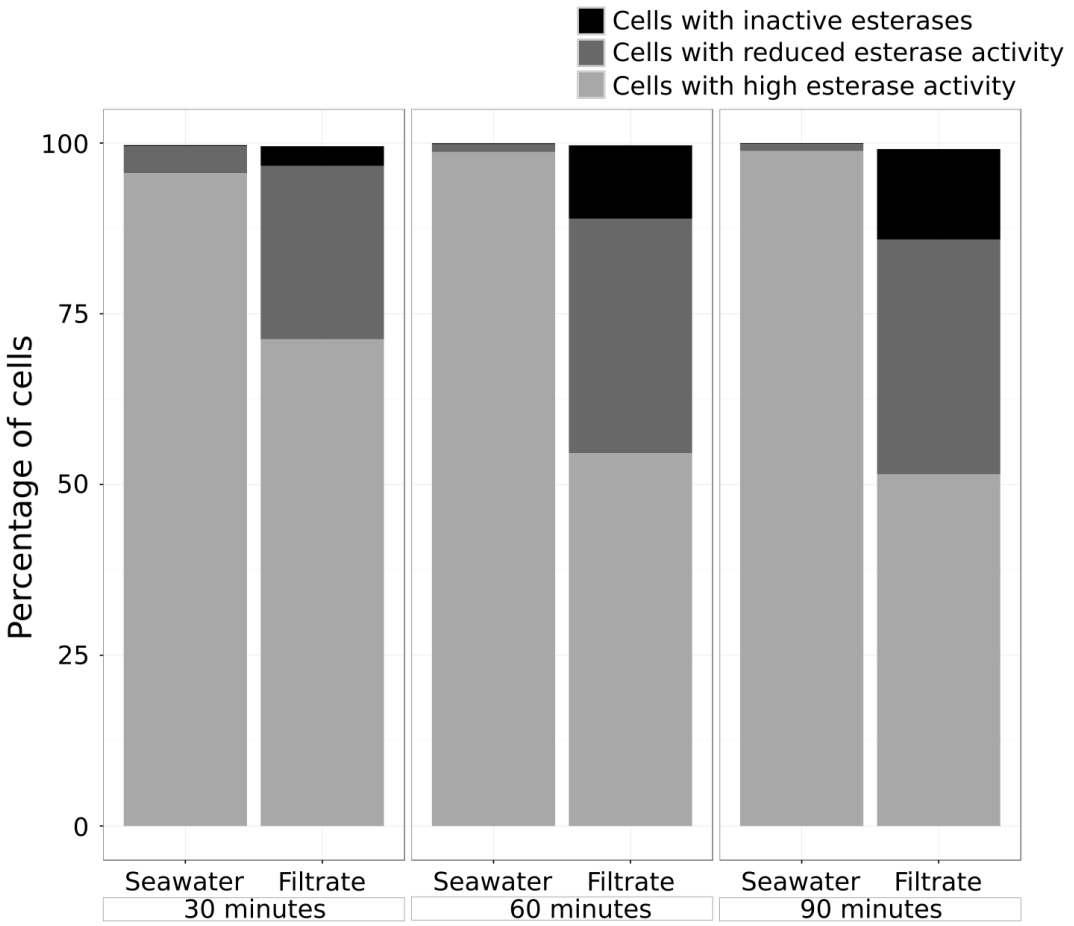

Figure 4: Metabolic activity of *C. muelleri* following exposure to control filtered seawater (seawater) or *A. minutum* filtrate (Filtrate) after 30, 60 and 90 min. Cells of *C. muelleri* are classified as cells with high esterase activity (light grey), reduced esterase activity (dark grey) and h inactive esterase (black).

3.3 Pigment composition

Among the 12 pigments identified, the amount (expressed as peak area) of 7 pigments significantly changed in the diatoms exposed to *A. minutum* filtrate (Table 1). Chlorophyll *a* (Chl *a*), chlorophyll C2 (Chl C2), diadinoxanthin (Ddx), and β-carotene decreased while allo-chlorophyll *a*, diatoxanthin (Dtx) and zeaxanthin (Zx) increased within 60 min of exposure. Changes occurred in pigments involved in xantophyll cycles with significant increases in zeaxanthin/violaxanthin (Zx/Vx) and diatoxanthin/diadinoxanthin (Dtx/Ddx) ratios. It is noteworthy that among six minor pigments that were quantified but not identified, three of them decreased significantly in the diatom exposed to filtrate (data not shown).

Table 1: Pigment composition expressed as peak area (peak area corresponding to 7 x 10^5 cells). Peak areas are expressed as mean ± standard deviation (n = 3). Statistical differences between seawater and filtrate are indicated as followed "•" 0.05 < p-value < 0.1, "*" 0.01 < p-value < 0.05, "**"0.001 < p-value < 0.01, "***" p-value < 0.001.

	30 min exposure		**60 min exposure**	

	Seawater	Filtrate	p-value	Seawater	Filtrate	p-value
Chl. *a*	2444 ± 138	2399.4 ± 102		2565 ± 101	2296 ± 27	*
Epi Chl. *a*	76 ± 27	70 ± 9		58 ± 9	48 ± 3	
Allo Chl. *a*	31 ± 11	39 ± 12		19 ± 0	47 ± 4	**
Chl. C1	781 ± 42	743 ± 18		736 ± 25	735 ± 6	
Chl. C2	834 ± 54	799 ± 53		893 ± 37	747 ± 10	*
Fucoxanthin	2781 ± 71	2771 ± 12		2801 ± 105	2600 ± 9	•
Diadinoxanthin	740 ± 3	499 ± 20	**	738.1 ± 22.5	479.1 ± 21.9	***
Diatoxanthin	94.6 ± 15.6	326.0 ± 22.3	***	102 ± 12	263 ± 11	***
Violaxanthin	12.5 ± 0.5	13 ± 1		14 ± 1	13 ± 1	
Zeaxanthin	20.4 ± 0.9	33 ± 1	***	21 ± 1	28.8 ± 0.9	***
Pheophytin *a*	6.7 ± 0.6	7.0 ± 0.4		7.2 ± 0.2	6.8 ± 0.1	•
β-carotene	263 ± 10	266 ± 4		272 ± 11	241 ± 5	*

Chl. *a*: Chlorophyll *a*, Allo Chl. *a*: Allo chlorophyll *a*, Chl. C1: Chlorophyll C1, Chl.C2: Chlorophyll C2.

3.4 Lipid class composition

After 30 min of filtrate exposure, there was no significant effect on the content of sterol esters, free sterols, triglycerides, alcohols and free fatty acids (FFA) (Table 2). After 60 min, the alcohol, sterol ester and free sterol content followed an increasing trend ($0.1 < \text{p-value} < 0.05$) while triglyceride (storage lipids) content followed a decreasing trend ($0.1 < \text{p-value} < 0.05$) in presence of filtrate. Phospholipids (phosphatidylinositol (PI), phosphatidylethanolamine (PE), phosphatidylcholine (PC) levels significantly decreased after 30 min ($\text{p-value} < 0.01$). After 60 min, the cellular PC remained lower in cells exposed to the filtrate than in control cells ($0.1 < \text{p-value} < 0.05$). Monogalactosyl-diacylglycerol (MGDG) was the only glycolipid effected by the filtrate (decreased after 30 min exposure; $\text{p-value} < 0.05$), whereas sulfoquinovosyl-diacylglycerol (SQDG) and digalactosyl-diacylglycerol (DGDG) were unaffected.

Table 2: Total (polar plus neutral) lipid classes composition (pg cell^{-1}) of *C. muelleri* exposed to seawater (control) or to *A. minutum* filtrate (Filtrate). Results are expressed as mean ± standard deviation.N = 3. Statistical differences between seawater and filtrate are indicated as followed "•" 0.05 < p-value < 0.1, "*" 0.01 < p-value < 0.05, "**"0.001 < p-value < 0.01.

	30 min exposure			60 min exposure		
	Seawater	Filtrate	p-value	Seawater	Filtrate	p-value
Sterol ester	0.08 ± 0.01	0.08 ± 0.02		0.08 ± 0.01	0.10 ± 0.01	•
Trigly.	10 ± 1	11.1 ± 0.8		12 ± 1	11.1 ± 0.8	•
FFA	0.29 ± 0.08	0.26 ± 0.04		0.4 ± 0.2	0.4 ± 0.2	
Alcohols	0.08 ± 0.01	0.08 ± 0.02		0.08 ± 0.01	0.10 ± 0.01	•
Free Sterols	0.26 ± 0.02	0.31 ± 0.03		0.29 ± 0.01	0.40 ± 0.06	•
PI	0.03 ± 0.00	0.05 ± 0.01	•	0.06 ± 0.02	0.05 ± 0.03	
PE	0.43 ± 0.06	0.38 ± 0.03		0.43 ± 0.03	0.41 ± 0.01	
PC	1.12 ± 0.02	0.61 ± 0.06	**	0.80 ± 0.09	0.6 ± 0.1	•
MGDG	2.2 ± 0.3	1.7 ± 0.1	*	2.0 ± 0.2	1.65 ± 0.09	
SQDG	1.2 ± 0.3	1.23 ± 0.08		1.38 ± 0.08	1.18 ± 0.09	
DGDG	0.25 ± 0.06	0.25 ± 0.02		0.28 ± 0.01	0.26 ± 0.02	
∑ lipids	16 ± 2	16 ± 1		17.9 ± 0.7	16.2 ± 0.9	

Trigly.: Triglyceride, FFA: Free fatty acids, PI: Phosphatidylinositol, PE: Phosphatidylethanolamine, PC: Phosphatidylcholine, MGDG: Monogalactosyl-diacylglycerol, SQDG, Sulfoquinovosyl-diacylglycerol, DGDG: Digalactosyl-diacylglycerol.

3.5 Fatty acid composition

Polar fatty acid composition was differed greatly when *C. muelleri* were exposed to seawater or to the allelochemicals after 30 min (global R: 1, significance = 0.09, ANOSIM) and 60 min (global R: 0.7, significance = 0.09, ANOSIM), with changes in the proportion of different fatty acids. The composition of neutral fatty acids was also differed greatly between seawater and filtrate exposures after 30 min (global R: 0.7, significance = 0.12, ANOSIM) and to a smaller extent after 60 min (global R: 0.48, significance = 0.09, ANOSIM). Overall, the presence of allelochemicals induced a decrease in the unsaturation index of polar lipids (Table 3) and in neutral FA content (Table 4). Polar FA composition change was observed within 30 min of filtrate exposure to the filtrate, while it took 60 min of exposure to the filtrate to modify the neutral FA composition. There were 8 fatty acids primarily effected by the allelochemicals, which accounted for 80% of differencies (Simper analysis) with controls. Filtrate exposure decreased the proportions of 22:6n-3, 20:4n-6, 20:5n-3, 16:3n-4, whereas the proportions of 18:1n-7, 16:1n-7, 16:0 and 14:0 were increased in presence of *A. minutum* filtrate (Figure 5).

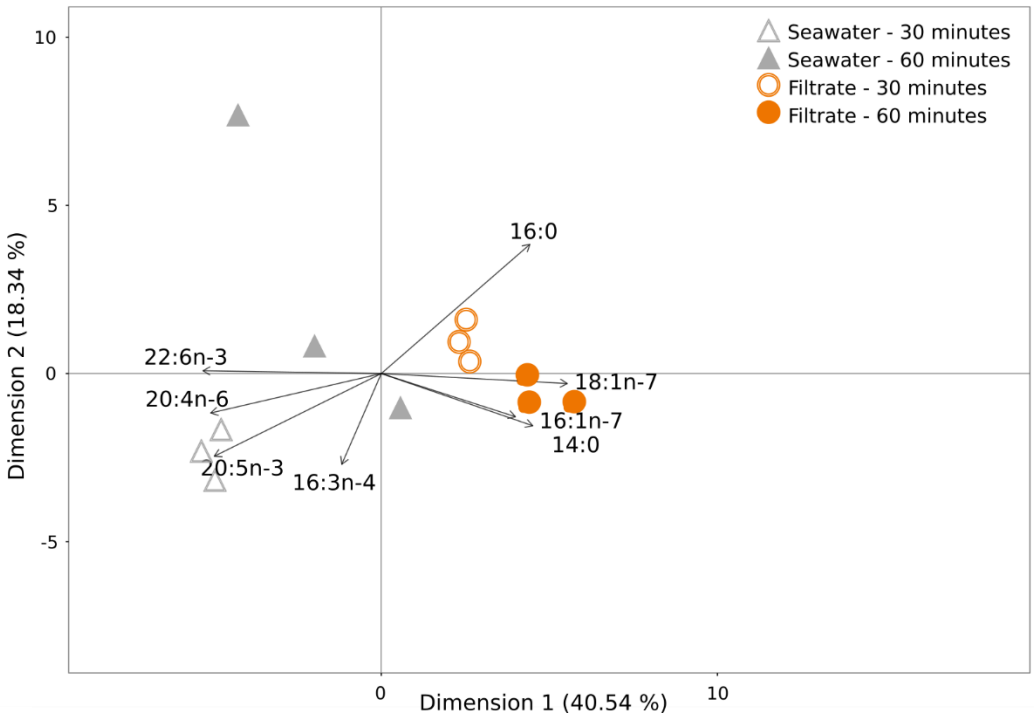

Figure 5: Principal component analysis (PCA) of polar fatty acid (FA) composition between *C. muelleri* cultures in presence of filtered seawater (grey triangles) or *A. minutum* filtrate (orange dots). Grey triangles represent samples exposed to filtered seawater after 30 min (empty triangles) and 60 min (filled triangles) of exposure. Orange dots represent samples exposed to *A. minutum* filtrate after 30 min (empty dots) and 60 min (filled dots). Dimension 1 represents 40.54% of variance and dimension 2 represents 18.34% of variance. FA shown explain 80% of differences (Simper analysis).

Table 3: Polar fatty acids (FA) composition (mass % of total polar fatty acids). The total mass (µg) correspond to the mass of 10^6 cells. Results are expressed as mean ± standard deviation (n = 3). P-value from the statistical tests between seawater and filtrate at each different time are indicated as followed "•" 0.05 < p-value < 0.1, "*" 0.01 < p-value < 0.05, "**"0.001 < p-value < 0.01, "***" p-value < 0.001.

	30 min exposure			60 min exposure		
	Seawater	**Filtrate**	**p-value**	**Seawater**	**Filtrate**	**p-value**
iso15:0	0.44 ± 0.02	0.68 ± 0.02	***	0.5 ± 0.1	0.75 ± 0.05	*
ant15:0	0.21 ± 0.02	0.26 ± 0.01	•	0.25 ± 0.07	0.31 ± 0.03	
iso17:0	0.64 ± 0.01	0.73 ± 0.00	**	0.75 ± 0.05	0.77 ± 0.05	
14:0	8.3 ± 0.3	8.8 ± 0.2	•	8.6 ± 0.8	9.0 ± 0.2	
15:0	0.58 ± 0.01	0.62 ± 0.01	**	0.61 ± 0.02	0.63 ± 0.03	
16:0	10.2 ± 0.1	11.1 ± 0.1	***	10.8 ± 0.2	11.02 ± 0.03	
18:0	1.22 ± 0.01	1.30 ± 0.01	**	1.5 ± 0.3	1.5 ± 0.2	
22:0	0.21 ± 0.01	0.23 ± 0.03		0.20 ± 0.06	0.21 ± 0.01	
24:0	0.2 ± 0.0	0.2 ± 0.2		0.17 ± 0.00	0.16 ± 0.01	•
∑ SFA	22.1 ± 0.3	24.1 ± 0.2	**	23.6 ± 0.6	24.5 ± 0.2	
16:1n-7	14.00 ± 0.2	14.7 ± 0.2	*	14.2 ± 0.6	14.4 ± 0.5	
16:1n-5	0.21 ± 0.01	0.22 ± 0.00	•	0.22 ± 0.00	0.23 ± 0.01	
18:1n-9	2.0 ± 0.1	1.93 ± 0.04		2.12 ± 0.05	1.90 ± 0.08	*
18:1n-7	2.98 ± 0.02	3.7 ± 0.1	*	3.2 ± 0.2	4.1 ± 0.3	**
18:1n-5	0.28 ± 0.03	0.34 ± 0.04	•	0.28 ± 0.05	0.37 ± 0.03	*
∑ MUFA	19.7 ± 0.2	21.24 ± 0.04	**	20.2 ± 0.7	21.3 ± 0.8	
16:2n-7	1.64 ± 0.02	1.73 ± 0.05	•	1.77 ± 0.03	1.78 ± 0.08	
16:2n-4	2.09 ± 0.04	2.15 ± 0.03		2.10 ± 0.05	2.2 ± 0.1	
16:3n-4	8.9 ± 0.2	8.4 ± 0.2	•	8.9 ± 0.2	8.9 ± 0.2	
16:4n-1	0.31 ± 0.01	0.27 ± 0.01	**	0.30 ± 0.01	0.30 ± 0.01	
18:2n-7	0.16 ± 0.00	0.18 ± 0.00	**	0.18 ± 0.00	0.18 ± 0.01	
18:2n-6	1.98 ± 0.02	1.91 ± 0.05		2.05 ± 0.03	1.79 ± 0.11	*
18:3n-6	6.14 ± 0.04	6.09 ± 0.16		6.3 ± 0.1	5.7 ± 0.4	•
18:4n-3	2.90 ± 0.00	2.78 ± 0.04	•	2.88 ± 0.08	2.74 ± 0.06	•
20:3n-6	0.22 ± 0.01	0.17 ± 0.00	***	0.22 ± 0.02	0.16 ± 0.01	*
20:4n-6	9.2 ± 0.2	8.2 ± 0.2	**	8.5 ± 0.1	7.5 ± 0.5	•
20:4n-3	0.18 ± 0.00	0.16 ± 0.01	*	0.15 ± 0.02	0.16 ± 0.00	
20:5n-3	20.2 ± 0.1	17.9 ± 0.2	***	18.0 ± 0.3	17.7 ± 0.1	
22:5n-6	0.18 ± 0.01	0.20 ± 0.00	*	0.20 ± 0.02	0.17 ± 0.03	
22:5n-3	0.14 ± 0.00	0.12 ± 0.00	**	0.14 ± 0.01	0.12 ± 0.00	
22:6n-3	3.06 ± 0.04	2.71 ± 0.12	*	2.9 ± 0.2	2.4 ± 0.2	*
∑ PUFA	57.5 ± 0.3	53.2 ± 0.4	***	54.8 ± 0.6	52.8 ± 0.4	*
Unsaturation index	230 ± 1	210 ± 2	***	216 ± 3	206 ± 2	*
Mass (µg)	490 ± 10	410 ± 50	.	446 ± 3	426 ± 86	

SFA: saturated fatty acids, MUFA: monounsaturated fatty acids, PUFA: polyunsaturated fatty acids.

Table 4: Neutral fatty acids (FA) composition (mass % of total neutral fatty acids). The total mass (µg) correspond to the mass of 10^6 cells. Results are expressed as mean ± standard deviation (n = 3). P-value from the statistical tests (student t test or wilcoxon test) between the conditions at each different time are indicated as followed "•" 0.05 < p-value < 0.1, "*" 0.01 < p-value < 0.05, "**"0.001 < p-value < 0.01.

	30 min exposure			60 min exposure		
	Seawater	**Filtrate**	**p-value**	**Seawater**	**Filtrate**	**p-value**
iso15:0	0.17 ± 0.02	0.17 ± 0.02		0.14 ± 0.04	0.21 ± 0.02	•
14:0	12.6 ± 0.2	12.6 ± 0.1		12.8 ± 0.2	12.8 ± 0.1	
15:0	0.98 ± 0.01	0.98 ± 0.00		0.97 ± 0.01	1.0 ± 0.1	
16:0	18.8 ± 0.2	18.5 ± 0.1		18.6 ± 0.2	18.3 ± 0.2	
18:0	1.69 ± 0.06	1.67 ± 0.06		1.68 ± 0.03	1.65 ± 0.04	
20:0	0.12 ± 0.01	0.11 ± 0.00		0.11 ± 0.00	0.11 ± 0.00	*
22:0	0.20 ± 0.00	019 ± 0.01		0.19 ± 0.01	0.17 ± 0.00	
24:0	0.21 ± 0.02	0.19 ± 0.01		0.21 ± 0.01	0.19 ± 0.02	
∑ SFA	35.0 ± 0.1	34.65 ± 0.09	*	34.9 ± 0.1	34.6 ± 0.3	
15:1n-5	0.19 ± 0.02	0.20 ± 0.02		0.16 ± 0.01	0.22 ± 0.00	**
16:1n-7	35.4 ± 0.2	35.01 ± 0.03	•	35.06 ± 0.05	34.82 ± 0.40	
16:1n-5	0.34 ± 0.00	0.35 ± 0.00		0.33 ± 0.00	0.34 ± 0.00	•
18:1n-9	0.81 ± 0.02	0.81 ± 0.01		0.79 ± 0.01	0.79 ± 0.01	
18:1n-7	0.36 ± 0.01	0.37 ± 0.01		0.35 ± 0.00	0.36 ± 0.00	
∑ MUFA	37.3 ± 0.2	36.89 ± 0.02	•	36.85 ± 0.08	36.7 ± 0.4	
16:2n-7	1.43 ± 0.02	1.46 ± 0.01		1.42 ± 0.02	1.47 ± 0.01	*
16:2n-4	0.92 ± 0.01	1.00 ± 0.02	**	0.95 ± 0.00	0.7 ± 0.6	
16:3n-4	1.14 ± 0.03	1.6 ± 0.1	*	1.29 ± 0.02	1.6 ± 0.1	*
16:3n-1	0.40 ± 0.03	0.42 ± 0.04		0.39 ± 0.02	0.48 ± 0.01	**
18:2n-6	0.87 ± 0.02	0.86 ± 0.00		0.86 ± 0.00	0.8 ± 0.1	
18:3n-6	3.17 ± 0.04	3.21 ± 0.01		3.12 ± 0.01	3.11 ± 0.05	
18:4n-3	2.02 ± 0.02	2.03 ± 0.02		1.99 ± 0.02	2.08 ± 0.02	**
20:3n-6	0.39 ± 0.01	0.38 ± 0.01		0.38 ± 0.00	0.37 ± 0.02	*
20:4n-6	4.86 ± 0.09	4.83 ± 0.09		5.03 ± 0.04	4.77 ± 0.09	*
20:4n-3	0.31 ± 0.01	0.30 ± 0.01		0.30 ± 0.01	0.30 ± 0.00	
20:5n-3	9.5 ± 0.2	9.61 ± 0.05		9.78 ± 0.04	9.7 ± 0.3	
22:5n-6	0.02 ± 0.00	0.02 ± 0.00		0.02 ± 0.00	0.02 ± 0.00	
22:5n-3	0.13 ± 0.01	0.12 ± 0.01		0.13 ± 0.00	0.12 ± 0.00	*
22:6n-3	0.58 ± 0.02	0.55 ± 0.02		0.56 ± 0.02	0.55 ± 0.01	
∑ PUFA	21.9 ± 0.3	21.9 ± 0.1		22.25 ± 0.03	22.0 ± 0.4	
Unsaturation index	107 ± 1	109.3 ± 0.2	*	109.6 ± 0.2	107 ± 2	
Mass (µg)	1121 ± 111	899 ± 47	•	1111 ± 142	746 ± 171	*

SFA: saturated fatty acids, MUFA: monounsaturated fatty acids, PUFA: polyunsaturated fatty acids.

4 Discussion

4.1 *Alexandrium minutum* allelochemicals are fast acting

This study demonstrated several significant effects (Figure 6) of *A. minutum* allelochemicals on the metabolism (decrease in esterase activity and increase in ROS production),

photosynthesis (decrease in maximum PSII quantum yield and increase of non-photochemical quenching) and membrane composition (changes in membrane lipids and pigments) in the diatom *C. muelleri* as compared to the controls. Overall, allelochemicals induced a decrease in metabolism within an hour, as highlighted by the inhibition of esterase activity and photosynthesis of the diatom *C. muelleri*, thus confirming that *A. minutum* allelochemicals are fast acting (Lelong et al., 2011; Tillmann et al., 2007). Moreover, this study highlights that photosynthesis was affected within a short time (< 30 min), as was the primary metabolism, as estimated by the esterase activity decrease after only 30 min. Indeed, 60 min was sufficient to almost completely cease esterase activity, down to 10% of the unexposedseawater control cells. This highlights the usefulness of analyzing cellular effects at a minute scale to elucidate the allelochemicals mode of action, which eventually lead to cell lysis. The combination of fluorescence, flow-cytometry and biochemical analysis of diatom physiology provided new insights on the short-term (within 30 min) cellular and biochemical mechanisms involved in allelochemical effects previously reported in *A. minutum* (Lelong et al., 2011) and *A. tamarense* (Ma et al., 2011; Zheng et al., 2016).

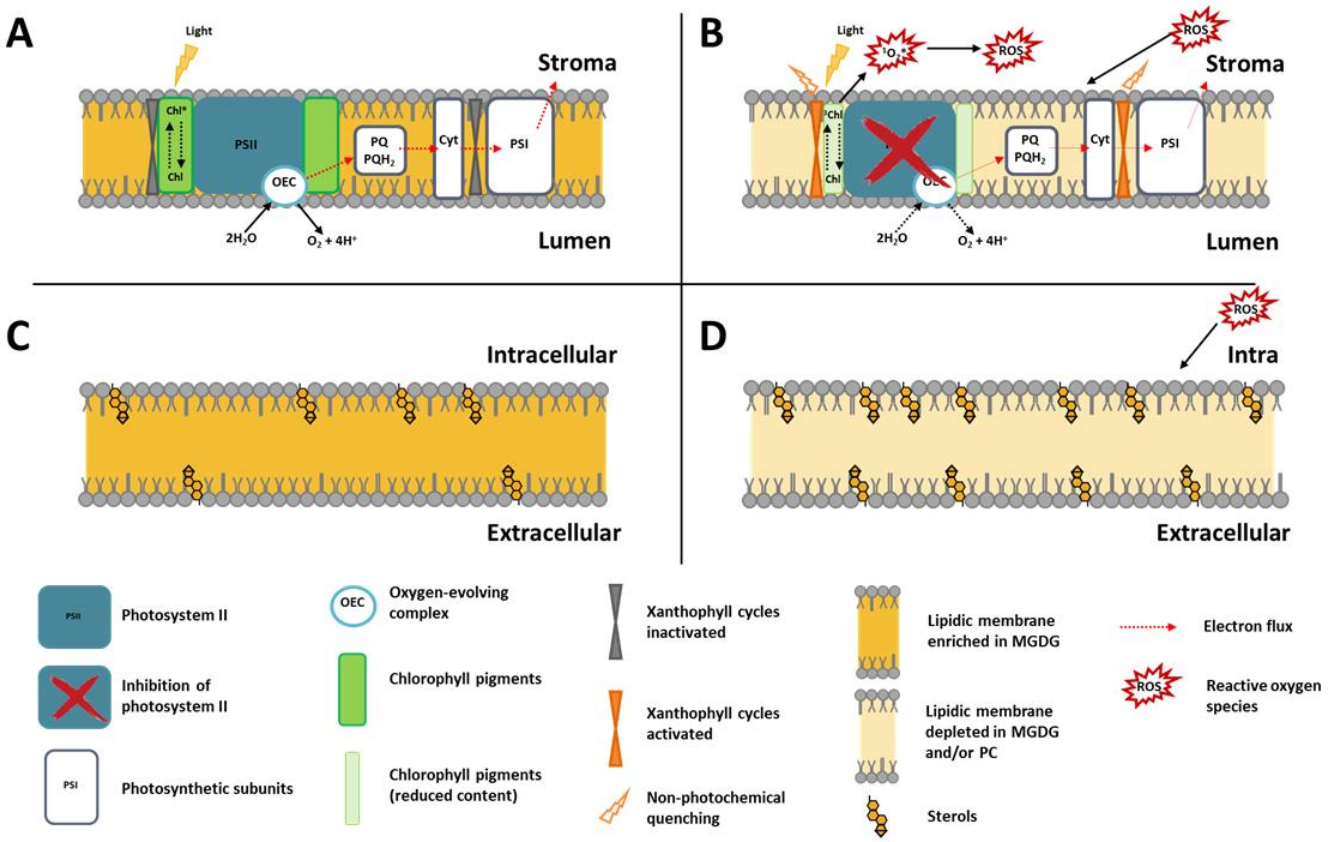

Figure 6 : Diagram of the mechanisms of *A. minutum* allelochemicals on photosynthetic (A and B) and cytoplasmic (C and D) membranes of *C. muelleri* in presence of seawater (A and C) and allelochemicals (B and D). Mechanisms are described in the last "general view" paragraph of discussion. PSII: Photosystem II, PSI: Photosystem I, PQ: Plastoquinone, Cyt, Cytochrome, OEC: Oxygen-evolving complex, Chl: Chlorophyll, PC: Phosphatidylcholine, MGDG: Monogalactosyl-diacylglycerol, ROS: Reactive oxygen species.

4.2 Effects of allelochemicals on photosystem II

A decrease in the maximum photosystem II (PSII) quantum yield (*Fv/Fm*) of *C. muelleri* was observed within 20 min of exposure to *A. minutum* filtrate, highlighting rapid deleterious effects to the PSII and supporting previous studies (Lelong et al., 2011; Tillmann et al., 2007). (Lelong et al., 2011) highlighted that the decrease of photosynthetic efficiency resulted from an inactivation of PSII reaction centers (RCs) and a decrease of electron transport through PSII. Inhibition of photosynthesis was also reported through a transcriptomic analysis of the diatom *Phaeodactylum tricornutum* when co-cultured for 24 h with an allelochemical strain of *A. tamarense* (Zheng et al., 2016). The authors hypothesized that the oxygen evolving complex (OEC) that catalyzes the oxidation of water to molecular oxygen was inhibited. This damage to PSII would result in an electron flux reduction through PSII and in the decreased quantum yield measured in our study. Effects of allelochemicals on the PSII of the diatom mimic the deleterious effects reported under excessive light intensity (i.e. photoinhibition). During photoinhibition, PSII are deactivated via two main steps: first OEC are damaged by light and deactivated, then PSII RCs are deactivated due to excess light absorption (Hakala et al., 2005; Nishiyama et al., 2006; Ohnishi et al., 2005). With less active RCs, the energy absorbed by chlorophyll pigments cannot be utilized for photochemistry (i.e. photosynthetic reactions) and accumulates, becoming an excess. Our results highlighted the deactivation of photosynthesis, however regardless of PSII inhibition, in presence of light, chlorophyll (Chl) pigments absorb photons and move to an excited state (^{1}Chl*). Excess light absorption can induce the production of toxic ^{3}Chl* that reacts with O_2 to produce the superoxide ion ($^1O_2$*), a highly reactive oxygen species (ROS) (Müller et al., 2001). Similarly, during our study a transitory increase of ROS production was observed upon exposure to *A. minutum* allelochemicals. The excess energy can be "safely" dissipated through fluorescence emission or heat dissipation (non-photochemical quenching; NPQ) as observed in our study and described below.

4.3 Effects of allelochemicals on pigments

Significant decreases in chlorophyll *a* and chlorophyll C2 content and red fluorescence (Fl3; 630 nm), in parallel with an increase in the chlorophyll (Chl) degradation product (allo-chlorophyll *a*) was observed after only 60 min of filtrate exposure (Figure 6 A and B). Bleaching (i.e. loss of cell pigmentation) of microalgal cells exposed to *Alexandrium* spp. filtrate has been previously reported (Lelong et al., 2011; Lyczkowski and Karp-Boss, 2014), and this phenomenon is likely related to a decrease of Chl content as reported here. Induction

of Chl degradation during allelochemical interactions has been recently shown (Yang et al., 2017; Zhou and Yu, 2006) and is a common photoacclimation process (Deblois et al., 2013; Dubinsky and Stambler, 2009; Sui and Han, 2014). We speculate that the decrease of Chl pigments results in a decrease in light harvesting antenna size. By decreasing the number of photons absorbed, the excess energy received by PSII would be decreased, mitigating photoinhibition and subsequent associated energy cost (Raven, 2011) as well as excessive ROS production and cell damages.

4.4 Effects of allelochemicals on non-photochemical quenching

Upon allelochemical exposure, the increase in non-photochemical quenching (NPQ) of *C. muelleri* is hypothesized to dissipate excess energy from damaged PSII through heat. Allelochemicals also induced a decrease in ß-carotene and changes in xanthophyll pigments ratios (diadinoxanthin/diatoxanthin and violaxanthin/zeaxanthin; Figure 6B) within photosynthetic membranes. Heat dissipation is mediated in thylakoid membranes by carotenoids and particularly xanthophyll pigment cycles (Goss and Jakob, 2010). The diadinoxanthin (Ddx) and violaxanthin (Vx) can be de-epoxidated in diatoxanthin (Dx) and zeaxanthin (Zx), respectively, to dissipate excess energy through heat emission (non-photochemical quenching; (Behrenfeld and Milligan, 2013; Goss and Jakob, 2010)). In the current study, activation of xanthophyll cycles, as demonstrated by increases in Dx/Ddx and Zx/Vx ratios, in the presence of allelochemicals was observed after both 30 and 60 min of filtrate exposure. While the increase in Dx was linked to a decrease in Ddx, Vx content did not change along with the increase in Zx content. *De novo* synthesis of Vx from β-carotene, a Vx precursor (Fraser and Bramley, 2004), may explain the homeostasis of Vx.

4.5 Effects of allelochemicals on lipids

The lipid composition of photosynthetic membranes, which physicochemical properties greatly influence NPQ and indeed diadinoxanthin (Ddx) and violaxanthin (Vx) de-epoxidation reactions (Latowski et al., 2011). These lipids were significantly affected by the presence of allelochemicals (Fig 6A and 6B). Monogalactosyldiacylglycerol (MGDG), a non-bilayer glycolipids exclusively found in thylakoid membranes, decreased in the presence of allelochemicals. Previous studies highlighted that MGDG allows xanthophyll solubilization and promotes de-epoxidation (Goss et al., 2009, 2005; Wilhelm et al., 2014). In parallel, a decrease in phosphatidylcholine (PC) content, a significant constituent of thylakoid

membranes (Kates, 1987; Lepetit et al., 2010; Vieler et al., 2007), was also observed in the presence of allelochemicals. Similar decreases of glycolipids along with a decrease in PC were observed during the photoinhibition process (Lepetit et al., 2010; Wilhelm et al., 2014). The modifications in the biochemical composition of photosynthetic membranes are another change similar to photoinhibition processes.

Changes in lipid class composition occurred alongside significant modifications in the fatty acid (FA) composition of both polar and neutral lipids. Filtrate of *A. minutum* reduced the cellular content of neutral fatty acids, mainly bound to storage lipids (i.e. triglyceride that represents more than 90% of neutral lipids), by more than 20% of its mass. This decrease in neutral FAs may be linked to the decrease in triglyceride and result from an energy mobilization to cope with the energy cost induced by allelochemicals such as lipid synthesis and de-epoxidation reactions, or from the mobilization of FAs for the synthesis of membrane FAs (Muhlroth et al., 2013). Exposure to *A. minutum* allelochemicals also reduced the unsaturation levels of polar lipid fatty acids which are the constituents of biological membranes. The decrease of membrane lipid unsaturation mainly results from the decreases of eicosapentaenoic acid (EPA) 20:5n-3 and 16:3n-4, accounting for 38% of total polar lipid FA. This decrease in polyunsaturated fatty acids (PUFA) paralleled the decrease in PC and MGDG, mainly constituted in 20:5n-3 and 16:3n-4, respectively (Da Costa et al., 2016; Guella et al., 2003; Li et al., 2014). In the diatom *Phaeodactylum tricornutum*, 20:4n-6 was only found associated to MGDG and PC and to a smaller extent to DGDG (Arao et al., 1987). Its decrease also occurred in parallel with the general decrease in PC and MGDG observed in the presence of allelochemicals. Concomitantly, proportions of other major FA (14:0, 16:0, 16:1n-7, 18:1n-7) increased.

Sterols are predominant constituents of plasma membranes (Hartmann and Benveniste, 1987; Hartmann, 1998) with many important roles including the regulation of membrane fluidity and permeability (Dufourc, 2008), signal transduction, modulation of enzyme activity and precursors of secondary metabolites (Hartmann, 1998). In microalgae, sterol can increase under increasing light (Gordillo et al., 1998; Piepho et al., 2010), indeed sterols may have a role under photoinhibition. The slight increase of sterols in the presence of filtrate, as observed under photoinhibition-like conditions, may confirm such a hypothesis. At the same time, some sterols classes are known to potentially act against antimicrobial compounds with membrane-disruptive activity (Dufourc, 2008; Mason et al., 2007). Authors have hypothesized that *A. tamarense* allelochemicals may be membrane-disruptive lytic compounds with a high affinity for sterols and that the molecular targets involve sterol

components (Ma et al., 2011). In the same study, the authors showed that allelochemicals had different affinities to different phytosterols and speculated that the composition of the outermost cellular membrane plays a role in tolerance to allelochemicals. Yet, in our study, sterols increased in presence of allelochemicals. While this may reflect a protective role of sterols, the true role of sterols in allelochemical interactions should be addressed in future studies as it could be a membrane feature driving allelochemical tolerance.

4.6 Effects of allelochemicals on ROS

Exposure of the diatom to *A. minutum* filtrate resulted in a relative increase in intracellular reactive oxygen species (ROS) during the first hour. Photosynthesis is one of the processes inducing ROS production that can damage photosystem II (Asada, 1999; Müller et al., 2001; Nishiyama et al., 2006). However, it is unlikely that the diatoms' photosystem II is the only source of ROS as a ROS increase was also reported in non-photosynthetic cells exposed to *A. minutum* exudates (Flores et al., 2012; Le Goïc et al., 2014). The two-fold ROS increase in *C. muelleri* exposed to allelochemicals may have led to some lipid peroxidation (yet to be measured). Lipid peroxides can act as a signal inducing programmed cell death (Yang et al., 2017) and cell cycle blockage (Farmer and Mueller, 2013) which was shown in *Phaeodactylum tricornutum* co-cultured with *A. tamarense* (Zheng et al., 2016), where ROS production returned to levels similar to control conditions after 90 min. While this decrease may be linked to the decrease in esterase activity, it is also hypothesized that diatoms may cope with ROS stress through activation of antioxidant systems (Li et al., 2015; Yang et al., 2017) such as xanthophyll pigments (Lepetit et al., 2012, 2010; Wilhelm et al., 2014), or through saturation of membranes. Xanthophyll pigments not only play a role in dissipation of energy, as mentioned above, but can also act as antioxidants, especially against ROS produced at PSII oxygen evolving complex (Wilhelm et al., 2014). Indeed, xanthophyll cycle may scavenge intracellular ROS induced by the presence of allelochemicals.

4.7 General view

Based on our results and previous studies (Lelong et al., 2011; Ma et al., 2011; Zheng et al., 2016) we propose a conceptual model to describe the mechanisms of action of *Alexandrium* spp. allelochemicals (Figure 6). Alteration of physiological functions such as photosynthesis and primary metabolism may result from direct damage to external membranes. Such damage may lead to the loss of cell integrity as shown by (Ma et al., 2011). Here we propose that the

membrane disruption observed by (Ma et al., 2011; Zheng et al., 2016) leads to an inhibition of photosynthesis. Membrane disruption was previously reported to lead to inhibition of *Fv/Fm* and electron transport (Yang et al., 2017). Following the inactivation of photosystem II, the energy trapped by chlorophyll pigments cannot be used for photochemistry. Thus photons become excessive within the cells and may induce an increase in ROS production by the cell. Photoinhibition-like processes appeared to be activated by the cells to mitigate the stress. The observed reduction of chlorophyll pigments is hypothesized to limit the energy trapped by the cell, together with the xanthophyll cycles to eliminate excess energy through heat (non-photochemical quenching) and to scavenge ROS. These changes of pigment content and ratio are accompanied by a decrease in MGDG and saturation of photosynthetic membranes. In parallel, plasma membranes were also modified as demonstrated by the increase in free sterols. While the role of sterols has yet to be investigated, they may help the cell to maintain membrane integrity and associated enzyme activity or act as protection mechanisms against membrane disruption. ROS increase is likely to be a key factor in understanding allelochemical interactions. Their origin, effects and role remain unclear, and the mechanisms involving ROS should be further studied. The main pending issues are to understand how the allelochemicals interact with cell membranes, and how it is related to the sensitivity of some species to better understand their ecological implications. Overall, the mode of action of allelochemicals has to be further investigated from the minute scale effects to fully understand the mechanisms leading to microalgal cell death.

5 Conclusion

In conclusion, our results bring new insights on allelochemical interaction mechanisms and indicate that several biochemical pathways and structures were rapidly impaired resulting in photoinhibition-like responses. Even though allelopathy does not automatically lead to cell death, sub-lethal effects, such as photoinhibition, ROS production, decreased metabolism or decreased energy absorption, would have a significant energy cost. For example, the cost of photoinhibition can lead to a decreased growth rate. Overall the allelochemical interactions would also impair the ability of the exposed cells to cope with other environmental stress, thus decreasing competitiveness and fitness. The sub-lethal markers reported here are valuable tools in assessing the importance and ecological roles of allelopathy in structuring plankton communities.

Acknowledgments

The authors kindly thank Nelly Le Goïc for the technical help and Dr. Bruno Jesus for the useful discussions. This study was carried out with the financial support of the National Research Agency (ANR) ‘‘ACCUTOX’’ project 13-CESA-0019 (2013–2017), the Région Bretagne, the University of Wollongong and the LabexMer.

References

Arao, T., Kawaguchi, A., Yamada, M., 1987. Positional distribution of fatty acids in lipids of the marine diatom *Phaeodactylum tricornutum*. Phytochemistry 26, 2573–2576. doi:10.1016/S0031-9422(00)83880-7

Arzul, G., Seguel, M., Guzman, L., Denn, E.E., 1999. Comparison of allelopathic properties in 3 toxic *Alexandrium* species. J. Exp. Bot. 232, 285 –295.

Asada, K., 1999. The water-water cycle in chloroplasts: scavenging of active oxygens and dissipation of excess photons. Annu. Rev. Plant Biol. 50, 601–639.

Behrenfeld, M.J., Milligan, A.J., 2013. Photophysiological Expressions of Iron Stress in Phytoplankton. Ann. Rev. Mar. Sci. 5, 217–246. doi:10.1146/annurev-marine-121211-172356

Blanco, J., Campos, M.J., 1988. The effect of water conditioned by a PSP producing dinoflagellate on the growth of four algal species used as food for invertebrates. Aquaculture 68, 289–298.

Borcier, E., Morvezen, R., Boudry, P., Miner, P., Charrier, G., Laroche, J., Hegaret, H., 2017. Effects of bioactive extracellular compounds and paralytic shellfish toxins produced by *Alexandrium minutum* on growth and behaviour of juvenile great scallops *Pecten maximus*. Aquat. Toxicol. 184, 142–154. doi:10.1016/j.aquatox.2017.01.009

Brookes, J.D., Geary, S.M., Ganf, G.G., Burch, M.D., 2000. Use of FDA and flow cytometry to assess metabolic activity as an indicator of nutrient status in phytoplankton. Mar. Freshw. Res. 51, 817–823. doi:10.1071/MF00048

Castrec, J., Soudant, P., Payton, L., Tran, D., Miner, P., Lambert, C., Goïc, N. Le, Huvet, A., Quillien, V., Boullot, F., Amzil, Z., Hégaret, H., Fabioux, C., 2018. Bioactive extracellular compounds produced by the dinoflagellate *Alexandrium minutum* are highly detrimental for oysters. Aquat. Toxicol. 199, 188–198. doi:10.1016/j.aquatox.2018.03.034

Chapelle, A., Le Bec, C., Le Gac, M., Labry, C., Amzil, Z., Guillou, L., Dreanno, C., Klouch, K., Siano, R., Pineau, L., Savar, V., Destombe, C., Dia, A., Lazure, P., Petton, S., Plus, M., Le Brun, L., Abernot, C., Duval, A., Doner, A., Gouriou, J., Gal, D. Le, Caradec, F., Andrieux, F., Malestroit, P., 2014. Étude sur la prolifération de la microalgue *Alexandrium minutum* en rade de Brest 61.

Da Costa, E., Silva, J., Mendonça, S.H., Abreu, M.H., Domingues, M.R., 2016. Lipidomic approaches towards deciphering glycolipids from microalgae as a reservoir of bioactive lipids. Mar. Drugs 14. doi:10.3390/md14050101

da Costa, F., Le Grand, F., Quéré, C., Bougaran, G., Cadoret, J.P., Robert, R., Soudant, P., 2017. Effects of growth phase and nitrogen limitation on biochemical composition of two strains of *Tisochrysis lutea*. Algal Res. 27, 177–189. doi:10.1016/j.algal.2017.09.003

Dalsgaard, J., John, M. St., Kattner, G., Müller-Navarra, D., Hagen, W., 2003. Fatty acid trophic markers in the pelagic marine environment, in: Southward, A.J., Tyler, P.A., Young, C.M., Fuiman, L.A. (Eds.), Advances in Marine Biology. Elsevier, pp. 227–318. doi:10.1017/CBO9781107415324.004

Deblois, C.P., Marchand, A., Juneau, P., 2013. Comparison of Photoacclimation in Twelve Freshwater Photoautotrophs (Chlorophyte, Bacillaryophyte, Cryptophyte and Cyanophyte) Isolated from a Natural Community. PLoS One 8. doi:10.1371/journal.pone.0057139

Dorsey, J., Yentsch, C.M., Mayo, S., McKenna, C., 1989. Rapid analytical technique for the assessment of cell metabolic activity in marine microalgae. Cytometry 10, 622–628. doi:10.1002/cyto.990100518

Dubinsky, Z., Stambler, N., 2009. Photoacclimation processes in phytoplankton: Mechanisms, consequences, and applications. Aquat. Microb. Ecol. 56, 163–176. doi:10.3354/ame01345

Dufourc, E.J., 2008. Sterols and membrane dynamics. J. Chem. Biol. 1, 63–77. doi:10.1007/s12154-008-0010-6

Farmer, E.E., Mueller, M.J., 2013. ROS-mediated lipid peroxidation and RES-activated signaling. Annu. Rev. Plant Biol. 64, 429–450. doi:10.1146/annurev-arplant-050312-120132

Flores, H.S., Wikfors, G.H., Dam, H.G., 2012. Reactive oxygen species are linked to the toxicity of the dinoflagellate *Alexandrium* spp. to protists. Aquat. Microb. Ecol. 66, 199–209. doi:10.3354/ame01570

Franklin, N.M., Adams, M.S., Stauber, J.L., Lim, R.P., 2001. Development of an improved rapid enzyme

inhibition bioassay with marine and freshwater microalgae using flow cytometry. Arch. Environ. Contam. Toxicol. 40, 469–480. doi:10.1007/s002440010199

Fraser, P.D., Bramley, P.M., 2004. The biosynthesis and nutritional uses of carotenoids. Prog. Lipid Res. 43, 228–265. doi:10.1016/j.plipres.2003.10.002

Garvey, M., Moriceau, B., Passow, U., 2007. Applicability of the FDA assay to determine the viability of marine phytoplankton under different environmental conditions. Mar. Ecol. Prog. Ser. 352, 17–26. doi:10.3354/meps07134

González-Fernández, C., Lacroix, C., Paul-Pont, I., Le Grand, F., Albentosa, M., Bellas, J., Viñas, L., Campillo, J.A., Hegaret, H., Soudant, P., 2016. Effect of diet quality on mussel biomarker responses to pollutants. Aquat. Toxicol. 177, 211–225. doi:10.1016/j.aquatox.2016.05.027

Gordillo, F.J.L., Goutx, M., Figueroa, F.L., Niell, F.X., 1998. Effects of light intensity , CO 2 and nitrogen supply on lipid class composition of *Dunaliella viridis* 135–144.

Goss, R., Jakob, T., 2010. Regulation and function of xanthophyll cycle-dependent photoprotection in algae. Photosynth. Res. 106, 103–22. doi:10.1007/s11120-010-9536-x

Goss, R., Lohr, M., Latowski, D., Grzyb, J., Vieler, A., Wilhelm, C., Strzalka, K., 2005. Role of hexagonal structure-forming lipids in diadinoxanthin and violaxanthin solubilization and de-epoxidation. Biochemistry 44, 4028–4036. doi:10.1021/bi047464k

Goss, R., Nerlich, J., Lepetit, B., Schaller, S., Vieler, A., Wilhelm, C., 2009. The lipid dependence of diadinoxanthin de-epoxidation presents new evidence for a macrodomain organization of the diatom thylakoid membrane. J. Plant Physiol. 166, 1839–1854. doi:10.1016/j.jplph.2009.05.017

Granéli, E., Hansen, P.J., Algal, H., Known, S., 2006. 15 Allelopathy in Harmful Algae : A Mechanism to Compete for Resources ? 15 . 2 Approaches to Demonstrate / Study Allelopathy – Pitfalls and Strength / Weaknesses of Experimental Approaches 189, 189–201.

Guella, G., Frassanito, R., Mancini, I., 2003. A new solution for an old problem: The regiochemical distribution of the acyl chains in galactolipids can be established by electrospray ionization tandem mass spectrometry. Rapid Commun. Mass Spectrom. 17, 1982–1994. doi:10.1002/rcm.1142

Guillard, R.R.L., 1975. Culture of phytoplankton for feeding marine invertebrates, in: Culture of Marine Invertebrate Animals. Springer, pp. 29–60.

Hakala, M., Tuominen, I., Keränen, M., Tyystjärvi, T., Tyystjärvi, E., 2005. Evidence for the role of the oxygen-evolving manganese complex in photoinhibition of Photosystem II. Biochim. Biophys. Acta - Bioenerg. 1706, 68–80. doi:10.1016/j.bbabio.2004.09.001

Hartmann, M.-A., Benveniste, P., 1987. Plant membrane sterols: Isolation, identification, and biosynthesis. Methods Enzymol. 148, 632–650.

Hartmann, M.A., 1998. Plant sterols and the membrane environment. Trends Plant Sci. doi:10.1016/S1360-1385(98)01233-3

Ianora, A., Boersma, M., Casotti, R., Fontana, A., Harder, J., Hoffmann, F., Pavia, H., Potin, P., Poulet, S.A., Toth, G., 2006. New trends in marine chemical ecology. Estuaries and Coasts 29, 531–551. doi:10.1007/BF02784281

Kates, M., 1987. Lipids of diatoms and of halophilic *Dunaliella* species, in: The Metabolism, Structure, and Function of Plant Lipids. Springer, pp. 613–621.

Latowski, D., Schaller, S., Olchawa-Pajor, M., Goss, R., Strzałka, K., 2011. Violaxanthin and diadinoxanthin cycles as an important photoprotective mechanism in photosynthesis. Russ. J. Plant Physiol. 58, 952–964. doi:10.1134/S1021443711060124

Le Goïc, N., Hégaret, H., Boulais, M., Béguel, J.P., Lambert, C., Fabioux, C., Soudant, P., 2014. Flow cytometric assessment of morphology, viability, and production of reactive oxygen species of *Crassostrea gigas* oocytes. Application to Toxic dinoflagellate (*Alexandrium minutum*) exposure. Cytom. Part A 85, 1049–1056. doi:10.1002/cyto.a.22577

Le Grand, F., Soudant, P., Siah, A., Tremblay, R., Marty, Y., Kraffe, E., 2014. Disseminated neoplasia in the soft-shell clam *Mya arenaria*: Membrane lipid composition and functional parameters of circulating cells. Lipids 49, 807–818. doi:10.1007/s11745-014-3917-4

Legrand, C., Rengefors, K., Fistarol, G.O., Granéli, E., 2003. Allelopathy in phytoplankton - biochemical, ecological and evolutionary aspects. Phycologia 42, 406–419. doi:10.2216/i0031-8884-42-4-406.1

Lelong, A., Haberkorn, H., Le Goïc, N., Hégaret, H., Soudant, P., 2011. A new insight into allelopathic effects of *Alexandrium minutum* on photosynthesis and respiration of the diatom *Chaetoceros neogracile* revealed by photosynthetic-performance analysis and flow cytometry. Microb. Ecol. 62, 919–930. doi:10.1007/s00248-011-9889-5

Lepetit, B., Goss, R., Jakob, T., Wilhelm, C., 2012. Molecular dynamics of the diatom thylakoid membrane under different light conditions. Photosynth. Res. 111, 245–257. doi:10.1007/s11120-011-9633-5

Lepetit, B., Volke, D., Gilbert, M., Wilhelm, C., Goss, R., 2010. Evidence for the Existence of One Antenna-Associated, Lipid-Dissolved and Two Protein-Bound Pools of Diadinoxanthin Cycle Pigments in Diatoms. Plant Physiol. 154, 1905–1920. doi:10.1104/pp.110.166454

Li, S., Xu, J., Chen, J., Chen, J., Zhou, C., Yan, X., 2014. The major lipid changes of some important diet microalgae during the entire growth phase. Aquaculture 428–429, 104–110. doi:10.1016/j.aquaculture.2014.02.032

Li, Y., Zhu, H., Lei, X., Zhang, H., Cai, G., Chen, Z., Fu, L., Xu, H., Zheng, T., 2015. The death mechanism of the harmful algal bloom species *Alexandrium tamarense* induced by algicidal bacterium *Deinococcus* sp. Y35. Front. Microbiol. 6. doi:10.3389/fmicb.2015.00992

Lima-Mendez, G., Faust, K., Henry, N., Decelle, J., Colin, S., Carcillo, F., Chaffron, S., Ignacio-Espinosa, J.C., Roux, S., Vincent, F., Bittner, L., Darzi, Y., Wang, J., Audic, S., Berline, L., Bontempi, G., Cabello, A.M., Coppola, L., Cornejo-Castillo, F.M., D'Ovidio, F., de Meester, L., Ferrera, I., Garet-Delmas, M.-J., Guidi, L., Lara, E., Pesant, S., Royo-Llonch, M., Salazar, G., Sánchez, P., Sebastian, M., Souffreau, C., Dimier, C., Picheral, M., Searson, S., Kandels-Lewis, S., Tara Oceans coordinators, Gorsky, G., Not, F., Ogata, H., Speich, S., Stemmann, L., Weissenbach, J., Wincker, P., Acinas, S.G., Sunagawa, S., Bork, P., Sullivan, M.B., Karsenti, E., Bowler, C., de Vargas, C., Raes, J., 2015. Ocean plankton. Determinants of community structure in the global plankton interactome. Science (80-.). 348, 1262073. doi:10.1126/science.1262073

Lyczkowski, E.R., Karp-Boss, L., 2014. Allelopathic effects of *Alexandrium fundyense* (Dinophyceae) on *Thalassiosira cf. gravida* (Bacillariophyceae): A matter of size. J. Phycol. 50, 376–387. doi:10.1111/jpy.12172

Ma, H., Krock, B., Tillmann, U., Bickmeyer, U., Graeve, M., Cembella, A., 2011. Mode of action of membrane-disruptive lytic compounds from the marine dinoflagellate *Alexandrium tamarense*. Toxicon 58, 247–258. doi:10.1016/j.toxicon.2011.06.004

Marie, D., Brussaard, C.P.D., Thyrhaug, R., Bratbak, G., Vaulot, D., 1999. Enumeration of marine viruses in culture and natural samples by flow cytometry. Appl. Environ. Microbiol. 65, 45–52.

Mason, A.J., Marquette, A., Bechinger, B., 2007. Zwitterionic phospholipids and sterols modulate antimicrobial peptide-induced membrane destabilization. Biophys. J. 93, 4289–4299. doi:10.1529/biophysj.107.116681

Morel, F.M.M., Rueter, J.G., Anderson, D.M., Guillard, R.R.L., 1979. Aquil: a chemically defined phytoplankton culture medium for trace metal tudies. J. Phycol. doi:10.1111/j.1529-8817.1979.tb02976.x

Moutel, B., Gonçalves, O., Le Grand, F., Long, M., Soudant, P., Legrand, J., Grizeau, D., Pruvost, J., 2016. Development of a screening procedure for the characterization of *Botryococcus braunii* strains for biofuel application. Process Biochem. 51, 1855–1865. doi:10.1016/j.procbio.2016.05.002

Muhlroth, A., Li, K., Rokke, G., Winge, P., Olsen, Y., Hohmann-Marriott, M.F., Vadstein, O., Bones, A.M., 2013. Pathways of lipid metabolism in marine algae, co-expression network, bottlenecks and candidate genes for enhanced production of EPA and DHA in species of chromista. Mar. Drugs 11, 4662–4697. doi:10.3390/md11114662

Müller, P., Li, X.P., Niyogi, K.K., 2001. Non-photochemical quenching. A response to excess light energy. Plant Physiol. 125, 1558–1566. doi:10.1104/pp.125.4.1558

Nishiyama, Y., Allakhverdiev, S.I., Murata, N., 2006. A new paradigm for the action of reactive oxygen species

in the photoinhibition of photosystem II. Biochim. Biophys. Acta - Bioenerg. 1757, 742–749. doi:10.1016/j.bbabio.2006.05.013

Ohnishi, N., Allakhverdiev, S.I., Takahashi, S., Higashi, S., Watanabe, M., Nishiyama, Y., Murata, N., 2005. Two-step mechanism of photodamage to photosystem II: Step 1 occurs at the oxygen-evolving complex and step 2 occurs at the photochemical reaction center. Biochemistry 44, 8494–8499. doi:10.1021/bi047518q

Piepho, M., Martin-Creuzburg, D., Wacker, A., 2010. Simultaneous effects of light intensity and phosphorus supply on the sterol content of phytoplankton. PLoS One 5, 1–7. doi:10.1371/journal.pone.0015828

Pohnert, G., 2010. Chemical noise in the silent ocean. J. Plankton Res. 32, 141–144. doi:10.1093/plankt/fbp118

Puglisi, M.P., Sneed, J.M., Sharp, K.H., Ritson-Williams, R., Paul, V.J., 2014. Marine chemical ecology in benthic environments. Nat. Prod. Rep. 31, 1510–1553. doi:10.1039/C4NP00017J

R Foundation for Statistical Computing, Vienna, A.I. 3-900051-07-0, 2011. R Development Core Team. R A Lang. Environ. Stat. Comput. 55, 275–286.

Ras, J., Claustre, H., Uitz, J., 2008. Spatial variability of phytoplankton pigment distributions in the Subtropical South Pacific Ocean: comparison between in situ and predicted data. Biogeosciences 5, 353–369. doi:10.5194/bgd-4-3409-2007

Raven, J.A., 2011. The cost of photoinhibition. Physiol. Plant. 142, 87–104. doi:10.1111/j.1399-3054.2011.01465.x

Strasser, J.R., Srivastava, A., Tsimilli-Michael, M., 2000. The fluorescence transient as a tool to characterize and screen photosynthetic samples, in: Probing Photosynthesis: Mechanism, Regulation & Adaptation. pp. 445–483.

Sui, N., Han, G., 2014. Salt-induced photoinhibition of PSII is alleviated in halophyte *Thellungiella halophila* by increases of unsaturated fatty acids in membrane lipids. Acta Physiol. Plant. 36, 983–992. doi:10.1007/s11738-013-1477-5

Tillmann, U., Hansen, P.J., 2009. Allelopathic effects of *Alexandrium tamarense* on other algae: Evidence from mixed growth experiments. Aquat. Microb. Ecol. 57, 101–112. doi:10.3354/ame01329

Tillmann, U., John, U., 2002. Toxic effects of *Alexandrium* spp. on heterotrophic dinoflagellates: an allelochemical defence mechanism independent of PSP-toxin content. Mar. Ecol. Prog. Ser. 230, 47–58. doi:10.3354/meps230047

Tillmann, U., John, U., Cembella, A., 2007. On the allelochemical potency of the marine dinoflagellate *Alexandrium ostenfeldii* against heterotrophic and autotrophic protists. J. Plankton Res. 29, 527–543. doi:10.1093/plankt/fbm034

Tillmann, U., Krock, B., Alpermann, T.J., Cembella, A., 2016. Bioactive compounds of marine dinoflagellate isolates from western Greenland and their phylogenetic association within the genus *Alexandrium*. Harmful Algae 51, 67–80. doi:10.1016/j.hal.2015.11.004

Touzet, N., Franco, J.M., Raine, R., 2007. Characterization of nontoxic and toxin-producing strains of Alexandrium minutum (Dinophyceae) in Irish coastal waters. Appl. Environ. Microbiol. 73, 3333–3342. doi:10.1128/AEM.02161-06

Van Heukelem, L., Thomas, C.S., 2001. Computer-assisted high-performance liquid chromatography method development with applications to the isolation and analysis of phytoplankton pigments. J. Chromatogr. A 910, 31–49. doi:10.1016/S0378-4347(00)00603-4

Vieler, A., Wilhelm, C., Goss, R., Rosmarie, S., 2007. The lipid composition of the unicellular green alga *Chlamydomonas reinhardtii* and the diatom *Cyclotella meneghiniana* investigated by MALDI-TOF MS and TLC 150, 143–155. doi:10.1016/j.chemphyslip.2007.06.224

Wilhelm, C., Jungandreas, A., Jakob, T., Goss, R., 2014. Light acclimation in diatoms: From phenomenology to mechanisms. Mar. Genomics 16, 5–15. doi:10.1016/j.margen.2013.12.003

Worden, A.Z., Follows, M.J., Giovannoni, S.J., Wilken, S., Zimmerman, A.E., Keeling, P.J., 2015. Rethinking the marine carbon cycle: Factoring in the multifarious lifestyles of microbes. Science (80-.). 347, 1257594–1257594. doi:10.1126/science.1257594

Yang, K., Chen, Q., Zhang, D., Zhang, H., Lei, X., Chen, Z., Li, Y., Hong, Y., Ma, X., Zheng, W., Tian, Y., Zheng, T., Xu, H., 2017. The algicidal mechanism of prodigiosin from *Hahella* sp. KA22 against *Microcystis aeruginosa*. Sci. Rep. 7, 7750. doi:10.1038/s41598-017-08132-5

Zheng, J.-W., Li, D.-W., Lu, Y., Chen, J., Liang, J.-J., Zhang, L., Yang, W.-D., Liu, J.-S., Lu, S.-H., Li, H.-Y., 2016. Molecular exploration of algal interaction between the diatom *Phaeodactylum tricornutum* and the dinoflagellate *Alexandrium tamarense*. Algal Res. 17, 132–141. doi:10.1016/j.algal.2016.04.019

Zhou, Y.H., Yu, J.Q., 2006. Allelochemicals and photosynthesis, in: Allelopathy: A Physiological Process with Ecological Implications. Springer, pp. 127–139. doi:10.1007/1-4020-4280-9_10